PHYSICAL REVIEW MATERIALS **1**, 034402 (2017)

Observation of unusual ferromagnetic cluster glass behavior in CrAlGe

M. U. Khan,[1,*] J. A. Brock,[1] A. Provino,[2,3] C. Belfortini,[2] and P. Manfrinetti[2,3]
[1]*Department of Physics, Miami University, Kreger Hall, Oxford, Ohio 45056, USA*
[2]*Department of Chemistry, University of Genova, Via Dodecaneso 31, 16146 Genova, Italy*
[3]*Institute SPIN-CNR, Corso Perrone 24, 16152 Genova, Italy*

(Received 4 May 2017; revised manuscript received 12 July 2017; published 10 August 2017)

We report on an experimental study on the structural and magnetic properties of the intermetallic compound CrAlGe. The material has been investigated in detail by x-ray diffraction, dc magnetization, ac susceptibility, and electrical resistivity measurements. X-ray diffraction and associated Rietveld analysis show that the compound crystallizes in the orthorhombic $TiSi_2$-type structure, with lattice parameters $a = 4.7531(1)$ Å, $b = 8.2182(1)$ Å, and $c = 8.6951(1)$ Å. The magnetization measurements demonstrate that the alloy is ferromagnetic with a Curie temperature of $T_C \approx 80$ K. At 5 K the magnetization saturates at 50 kOe with a saturation moment of $M_S = 19$ emu/g. Below T_C, the ac susceptibility data exhibit two distinct frequency dependent peaks, which are also strongly dependent on ac field amplitude and dc magnetic fields. The experimental results strongly suggest the coexistence of ferromagnetic and reentrant spin glass type states in CrAlGe, which is due to the effect of the structural disorder in the $16f$ site (mixed Al/Ge occupation) on the crystallographically ordered $8a$ site of Cr. To our knowledge, CrAlGe is the first example where such unusual magnetic behavior is brought about not by structural disorder on the site occupied by the magnetic atom, but is due to the disorder in the atomic sites of the neighboring atoms.

DOI: 10.1103/PhysRevMaterials.1.034402

I. INTRODUCTION

The $3d$ transition metal Cr exhibits a large magnetic moment of $5\,\mu_B$ in its atomic form. However, Cr is antiferromagnetic with a small magnetic moment of $0.6\,\mu_B$ in its condensed bcc elemental form [1]. Interestingly, the Stoner theory of ferromagnetism suggested that in the hexagonal close packed (hcp) phase Cr is ferromagnetic [2]. The results of a theoretical approach based on self-consistent linear muffin-tin orbital calculations also supported this idea and showed a weak ferromagnetic ground state for hcp Cr, with a magnetic moment of $0.1\,\mu_B$ per Cr atom [3]. An experimental observation of a weak ferromagnetic state of hcp Cr was reported by Albrecht *et al.* in multilayered thin films of Cr/Ru (0001) [4]. Following this observation, ferromagnetism was also reported in the tetragonally distorted α phase of Cr [5]. Considering these observations, it is interesting to explore ferromagnetism in Cr containing alloys.

Recently, Yoshinaga *et al.* [6] and Fukuda *et al.* [7] reported the magnetic and structural properties of CrAlGe. The material exhibited an orthorhombic $TiSi_2$-type structure and showed ferromagnetism with a Curie temperature of $T_C = 80$ K. At 5 K, the spontaneous magnetic moment, saturation magnetic moment, and effective magnetic moment were found to be $M_0 = 0.41\,\mu_B/\text{f.u.}, M_S = 0.45\,\mu_B/\text{f.u.}$, and $M_{\text{eff}} = 1.89\,\mu_B/\text{f.u.}$, respectively. It was suggested that CrAlGe is a weak itinerant electron ferromagnet. The study of CrAlGe was motivated by the magnetic properties of MnAlGe, which is a ferromagnetic compound with a T_C of 518 K and, unlike CrAlGe, exhibits a Cu_2Sb-type tetragonal structure [8–10]. The material demonstrated a spontaneous magnetic moment of $3.25\,\mu_B/\text{f.u.}$ along with a large c-plane uniaxial magnetic anisotropy. Interestingly, when Mn was partially replaced by Cr in $Mn_{1-x}Cr_xAlGe$ ($x \leqslant 0.2$) both the T_C and spontaneous magnetization increased for the system [9,10]. Therefore, one would expect the T_C of CrAlGe to be much higher than 80 K. However, the experimental results discussed above showed otherwise.

Considering the discussion above, it is interesting to further explore the magnetic properties of CrAlGe. Therefore, in this paper we report on an experimental study on the structural and magnetic properties of CrAlGe. Interestingly, our results show that the material exhibits reentrant spin glass behavior. Materials exhibiting frustrated magnetic behavior are of great interest and have been extensively studied for many years [11–15]. In some materials, such frustrations in magnetic exchange interaction results in a spin glass (SG) state. In stoichiometric ordered compounds, SG behaviors are rarely observed. Therefore, the investigation of SG states caused by magnetic frustration is one of the most interesting topics in magnetism. SGs are magnetic systems in which the interactions between the magnetic moments are “in conflict” with each other due to some frozen-in structural disorder. Thus, no conventional long-range order (either of ferromagnetic or antiferromagnetic type) can be established. Nevertheless these systems exhibit a “freezing transition” to a state with a new kind of “order” in which the spins are aligned in random directions. The study of the spin ordering behavior in spin glasses constitutes a typical problem belonging to the physics of structurally disordered materials; such phenomena do not arise in more conventional regular systems such as ideal crystals [16]. Systems which exhibit SG characteristics at temperatures below the ferromagnetic Curie temperature T_C are often referred to as reentrant spin glasses (RSG) or cluster spin glasses [14,15].

The experimental results for CrAlGe strongly suggest that the spin glass behavior in the material is not due to any structural disorder on the site occupied by the magnetic atom, but caused by the disorder in the atomic sites of the neighboring

---

[*] Corresponding author: khanm2@miamioh.edu

2475-9953/2017/1(3)/034402(8)

atoms. To the best of our knowledge, this is the first observation of such magnetic behavior in a material where the magnetic atom occupies a single crystalline site.

II. EXPERIMENTAL TECHNIQUES

Approximately 3 g of polycrystalline sample of CrAlGe was prepared by arc melting technique using commercial high purity metals (99.99 wt. % for Cr; 99.999 wt. % for both Al and Ge). The elements, weighed in stoichiometric amounts (Cr in granules, Al in chunks cut from a rod, and Ge in pieces) were melted in a pure Ar atmosphere (TiZr gettered). The button was remelted five times after turning it upside down each time (total weight loss was 0.6 wt. %). The alloy did not form properly during the arc melting process, as drops of liquid Al leaked from the ingot surface after the first solidification. Therefore, to promote homogenization and proper crystallization, the as casted sample was wrapped in an outgassed Ta foil and was sealed in a quartz ampoule under vacuum for thermal treatment. After the temperature was raised to 700 °C in 6 h, it was annealed at 850 °C for 10 days followed by air cooling to room temperature. The resulting alloy was microcrystalline, brittle, stable in air, and with ash-gray color.

The structure and phase purity analysis of the sample was performed using micrographic examination and x-ray powder diffraction. Micrographic observation was performed by both optical (LOM) and electron microscopy (SEM), the latter equipped with a microprobe (EDS) for semiquantitative phase analysis (counting times of 60 s). As shown in the micrographs in Fig. 1, the sample is single phase and contains no impurity phase. Structural characterization was performed using both a Guinier camera [Cu $K\alpha1$ radiation; Si as an internal standard, $a = 5.4308(1)$ Å] and a Philips diffractometer (Cu $K\alpha1$ radiation) for data collection (2θ range of 5°–105°, in steps of 0.02° and a counting time of 24 s/step). The Guinier powder pattern was indexed using LAZY PULVERIX [17]; accurate lattice parameters were obtained by a least-squares program. The Rietveld refinement of the crystal structure was performed using the FULLPROF program [18].

Magnetization, ac susceptibility, and resistivity measurements were performed on a Physical Property Measurement System (PPMS) made by Quantum Design Inc. The magnetization measurements were performed as a function of both temperature (in the range 5–300 K) and applied magnetic field (up to 50 kOe). The ac susceptibility measurements were performed in the temperature range of 5–300 K in an ac field of 15 Oe and at various frequencies. The electrical resistance was measured as a function of temperature between 5 and 300 K in zero magnetic field.

III. RESULTS AND DISCUSSION

A. Crystal structure of CrAlGe

The existence of this compound was earlier reported in a work concerning the Cr-Al-Ge ternary system (isothermal section at 600 °C) [19]. In this work the CrAlGe compound was found to be stoichiometric and crystallizing in the orthorhombic $TiSi_2$ structure type (Pearson symbol $oF24$, space group $Fddd$, No. 70, $Z = 8$), with lattice parameters $a = 4.750(8)$ Å, $b = 8.224(2)$ Å, $c = 8.695(2)$ Å. The structure of this prototype presents two Wyckoff sites, the $8a$ and $16f$ for Ti and Si atoms, respectively [20,21]. In the literature, a restricted number of intermetallic compounds have been reported to adopt this type of structure. These include the binary compounds formed between a transition metal (Ti, Zr, Os, Ru) and Al and Ga or Si and Ge, and the ternary compounds formed between a transition metal (Cr, Mn, Mo, Nb) with Al (Ga) and Si (Ge) [22,23].

X-ray powder diffraction and Rietveld refinement of the crystal structure confirm that the CrAlGe compound crystallizes in the orthorhombic $TiSi_2$-type structure ($oF24$, $Fddd$). The lattice parameters, as obtained from the Guinier pattern, are $a = 4.754(2)$ Å, $b = 8.222(3)$ Å, and $c = 8.699(3)$ Å [observed unit cell volume $V_U = 340.02(1)$ Å^3]. The plot of the Rietveld refinement is shown in Fig. 2; the atomic coordinates

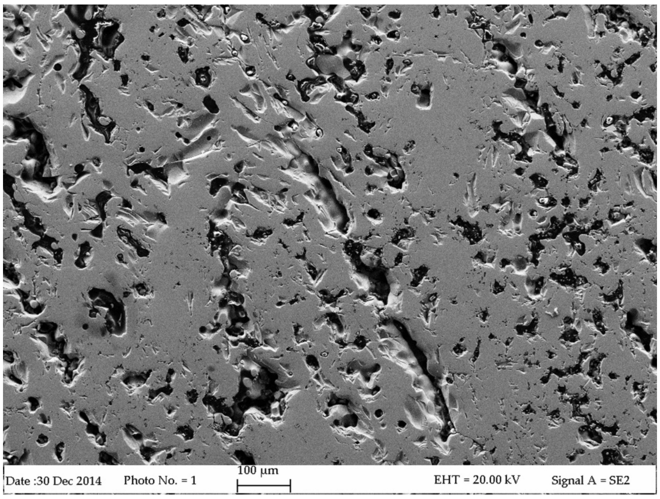

FIG. 1. SEM micrograph [backscattered electron (BSE) mode] of the CrAlGe sample used for physical measurements; the image shows a single phase material with a large volume fraction of annealing voids.

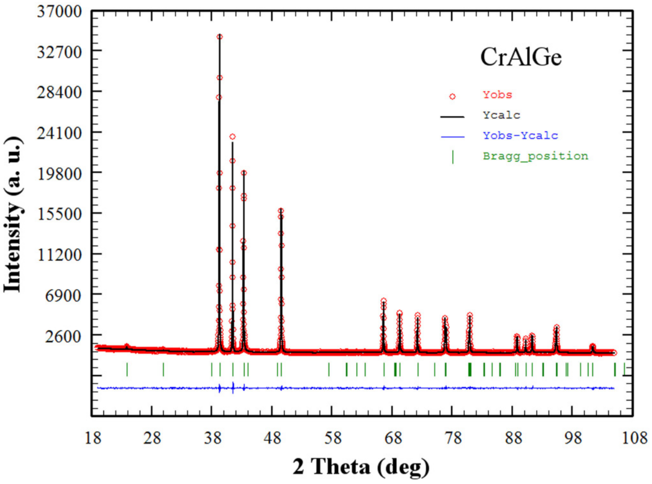

FIG. 2. Observed x-ray powder pattern (red circle) and Rietveld refinement profile (black line) of the CrAlGe compound. The blue line is the difference between observed and calculated data; the vertical bars (green) indicate the Bragg angle positions.

TABLE I. Atomic coordinates for the CrAlGe compound [orthorhombic $TiSi_2$-type, $oF24$, $Fddd$ (No. = 70)] as obtained from Rietveld method [refined formula $CrAl_{1.01(2)}Ge_{0.99(2)}$].[a]

		Atomic coordinates				
Atom	Wyckoff site	x	y	z	Occ.	B_{iso}(Å^2)
Cr	$8a$	1/8	1/8	1/8	1	0.13(7)
Al	$16f$	1/8	0.4551(1)	1/8	0.5063(2)	0.24(4)
Ge	$16f$	1/8	0.4551(1)	1/8	0.4937(2)	0.24(4)

[a] $a = 4.7531(1)$ Å, $b = 8.2182(1)$ Å, $c = 8.6951(1)$ Å, $V_U = 339.65(1)$ Å^3. $R_B = 0.87\%$, $R_{wp} = 7.77\%$, $\chi^2 = 0.90$.

are reported in Table I while the interatomic distances are listed in Table II. Rietveld refinement shows that the Cr atom fills the crystallographic site $8a$, which is occupied by Ti in the $TiSi_2$ prototype. Al and Ge atoms occupy, with a partial occupation (Al/Ge), the Wyckoff site $16f$ (with an occupation factor of 0.5 for each, respectively); this site is filled by Si in $TiSi_2$. The crystal structure of CrAlGe is built of closed packed hexagonal layers parallel to the a-b plane with composition $Cr(Al/Ge)_2$; within each layer Cr lies at the center of the hexagon while the Al/Ge atoms are located at the corners. The unit cell contains four layers (interlayer distance of $c/4$); these layers are stacked on top of each other and shifted apart to allow Cr atoms of adjacent layers to avoid a closer contact. The structure is compact and typical to that of an intermetallic compound. Projections along the a and c axis are represented in Figs. 3(a) and 3(b), respectively. A perspective view of the crystal structure is shown in Fig. 4(a). Similar structures, formed by layers stacked in different sequences, are the $CrSi_2$- and $MoSi_2$-types; their occurrence appears to be governed by electron-valence rules [24,25].

The shortest interatomic distances d_{obs}, corresponding to the first gap in the values of $d_{obs}/\Sigma r_M$ (where Σr_M is the sum of the two atomic radii), i.e., $d_{obs}/\Sigma r_M \leqslant 1.20$, can be considered as bond distances. Among the several bond distances, the bonds formed between Cr and Al/Ge atoms (2.563 Å) are shorter and stronger than those formed between Al/Ge-Al/Ge atoms (2.585 Å). A weak bond is formed between Cr atoms, with a distance of 3.218 Å which is slightly but clearly higher than the sum of Cr metallic radii (2.720 Å) [26]. Evaluation of the interatomic distances and chemical bonds (Table II) leads to the identification of the coordination spheres and determination of the atomic coordination number

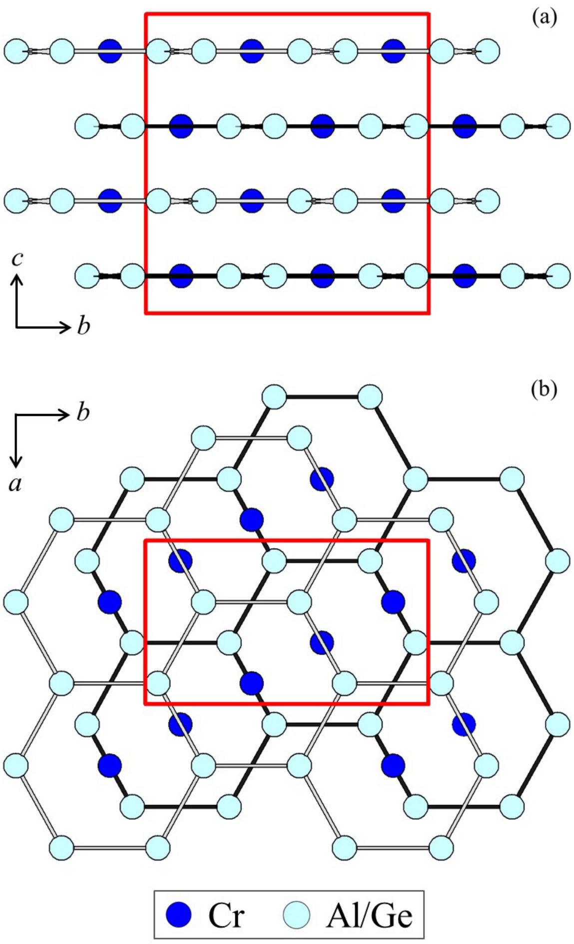

FIG. 3. The crystal structure of CrAlGe. Projections along the a axis (a) and the c axis (b). Colorless bond distances are for atoms set at $z = 3/8$ and $7/8$, while the black bond distances are for atoms at $z = 1/8$ and $5/8$.

TABLE II. Interatomic distances and coordination number (CN) in CrAlGe compound for $d_{obs}/\Sigma r_M \leqslant 1.20$ [orthorhombic $TiSi_2$-type, $oF24$, $Fddd$ (No. = 70)].

Central atom	Ligands	d (Å)	$d_{obs}/\Sigma r_M$	Polyhedron
Cr-	4 Cr	3.218	1.183	Rhombic dodecahedron CN = 14 $Cr@Cr_4(Al/Ge)_{10}$
	2 Al/Ge	2.713	0.983	
	4 Al/Ge	2.756	0.998	
	4 Al/Ge	2.563	0.929	
(Al/Ge)-	1 Cr	2.713	0.983	Rhombic dodecahedron CN = 14$(Al/Ge)@Cr_5(Al/Ge)_9$
	2 Cr	2.756	0.998	
	2 Cr	2.563	0.929	
	1 Al/Ge	2.792	0.997	
	2 Al/Ge	2.717	0.970	
	2 Al/Ge	2.585	0.923	
	4 Al/Ge	3.218	1.150	

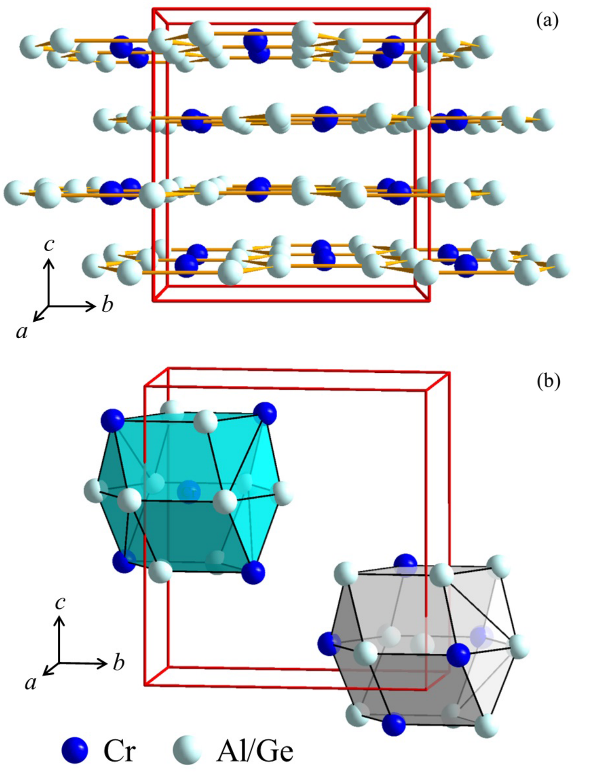

FIG. 4. A perspective view of the crystal structure, formed by hexagonal layers of composition Cr(Al/Ge)$_2$ stacked along the c axis (a). The two rhombododecahedral coordination polyhedra surrounding Cr and Al/Ge atoms (both atoms with CN = 14); their compositions are Cr$_4$(Al/Ge)$_{10}$ and Cr$_5$(Al/Ge)$_9$, for Cr and Al/Ge, respectively (only the two representative polyhedra are shown, all other atoms are not) (b).

(CN) and polyhedra surrounding Cr and Al/Ge atoms. The coordination polyhedron is a rhombic dodecahedron for both Cr and Al/Ge atoms, with CN = 14; its composition is Cr$_4$(Al/Ge)$_{10}$ and Cr$_5$(Al/Ge)$_9$ for Cr and Al/Ge, respectively [Fig. 4(b)]. If only Cr atoms are taken into account and the shortest Cr-Cr distance is considered, each Cr atom is found to be at the center of a regular tetrahedron (CN = 4) where all four Cr atoms are at the same distance of 3.218 Å from the central atom. The Cr-Cr intralayer interatomic distance is 4.747 Å, which is too large to be a bond distance. Figure 5 shows a sketch of the Cr sublattice in CrAlGe.

B. Magnetic and transport properties

The temperature dependence of the dc magnetization $M(T)$ of CrAlGe obtained at various magnetic fields, under ZFC and FC conditions, is shown in Fig. 6. As shown in Fig. 6(a), for a magnetic field of 25 Oe, the ZFC $M(T)$ data show negative magnetization at low temperatures. The magnetization increases nonlinearly in the positive direction with increasing temperature and peaks at $\sim$76 K. With further increase of temperature the magnetization decays following the Curie-Weiss law. The FC and ZFC $M(T)$ data overlap above 76 K, while below this temperature the two data demonstrate thermomagnetic irreversibility. As also shown in Fig. 6, such irreversibility below 76 K is observed in the ZFC and FC

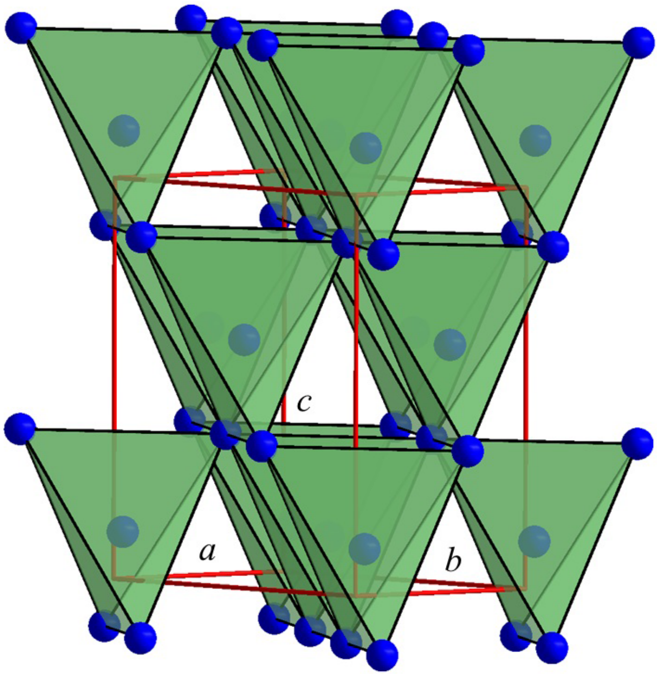

FIG. 5. A sketch of Cr sublattice, built up by corner-sharing Cr@Cr4 tetrahedra. Al/Ge atoms are not shown (for simplicity).

$M(T)$ data obtained at all magnetic fields ($H \leqslant 100$ Oe). However, the ZFC magnetization at low temperatures shifts towards the positive direction with increasing magnetic field. For $H > 50$ Oe, the ZFC data for all fields shows a positive magnetization. The negative value of the ZFC magnetization at low temperatures is due to the sample being cooled in a net negative trapping field, which was present above the superconducting solenoid. Such trapping field commonly exists in the PPMS superconducting magnet [27]. A T_C of $\approx$80 K was determined from derivative of the $M(T)$ data obtained at $H > 50$ Oe, which is consistent with the literature value [6]. The trend in the low field $M(T)$ discussed above is indicative of ferromagnetic cluster glass behavior in CrAlGe [13].

The plots for the $M(T)$ data obtained at higher magnetic fields are shown in Fig. 7. For all magnetic fields ($1 \leqslant H \leqslant 50$ kOe) the material show typical ferromagnetic behavior, where the ferromagnetic transition apparently shifts to higher temperature with increasing magnetic field. This is an expected behavior for a second order ferromagnetic-paramagnetic phase transition. Ferromagnetism is also observed in the $M(H)$ data of the compound obtained at 5 K (Fig. 8), which shows that the magnetization nearly saturates at 50 kOe with a saturation moment of $M_S \approx 15$ emu/g (0.42 μ_B/f.u.). The observed M_S is consistent with the value reported in literature [6]. As shown in the inset of Fig. 8, the CrAlGe compound exhibits a coercivity H_C of $\approx$170 Oe.

Figure 9 shows the temperature dependence of the real (χ') and imaginary (χ'') components of the ac susceptibility data for CrAlGe. The measurements were performed at an ac field of $H_{ac} = 15$ Oe and at various frequencies ranging from 10 Hz–10 kHz. As shown in Fig. 9(a), the $\chi'(T)$ data obtained at 10 Hz exhibit a broad peak near 50 K. While the peak is strongly suppressed as the frequency is increased [see inset of

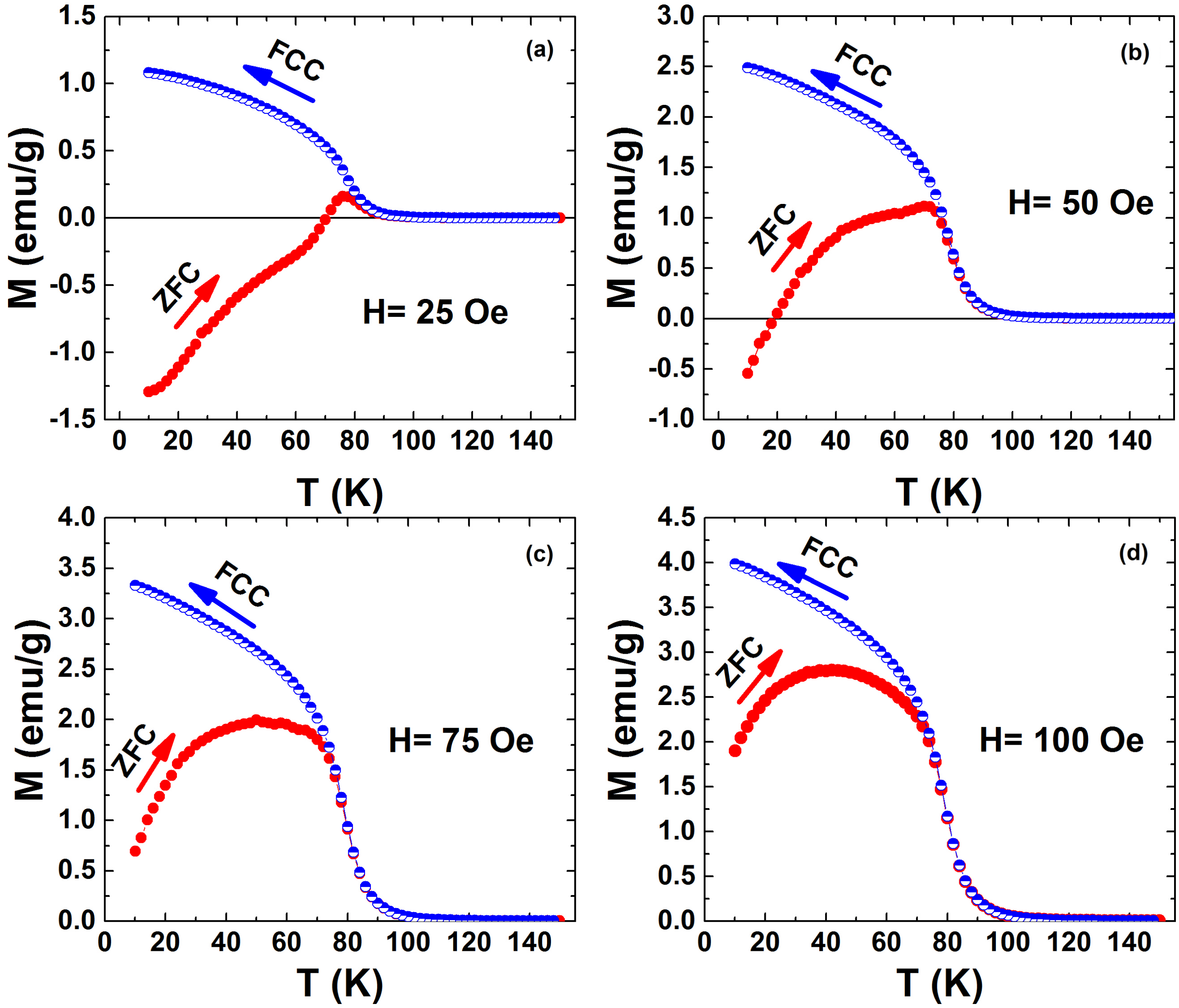

FIG. 6. dc magnetization vs temperature for CrAlGe measured between 5 and 150 K at (a) 25 Oe, (b) 50 Oe, (c) 75 Oe, and (d) 100 Oe.

Fig. 9(a) for a clearer view], no change was observed in the peak temperature. A second (much sharper) peak of relatively higher magnitude is observed at ≈76 K for a frequency of 10 Hz, which is consistent with peak temperature of the $M(T)$ data obtained at 25 Oe [see Fig. 6(a)]. With increasing frequency the magnitude of the peak is significantly suppressed and shifts to higher temperature (79 K for a frequency of 10 kHz).

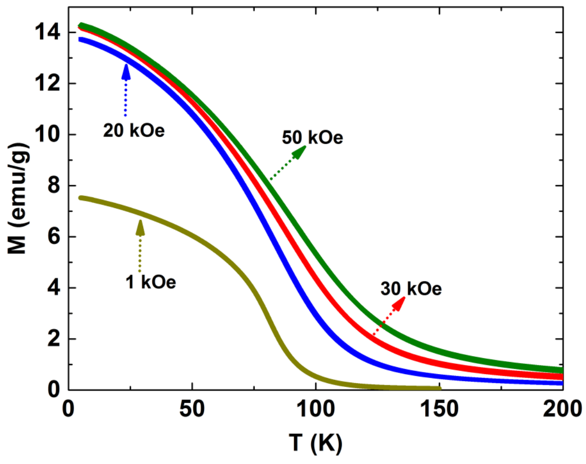

FIG. 7. dc magnetization vs temperature for CrAlGe measured at various magnetic fields.

The $\chi''(T)$ data [Fig. 9(b)] exhibits similar behavior with the exception that the frequency dependence of the data near 50 K is more significant when compared to the $\chi'(T)$ data. It is also interesting to note that while the sharp peak in the $\chi'(T)$ data was observed at ≈76 K, the same is observed at a lower temperature of ≈73 K in the $\chi''(T)$ data. The peak is suppressed with increasing frequency and shifts to ≈77 K for $f = 10\,\text{kHz}$ [see inset of Fig. 9(b) for a clear view]. The frequency dependence of the ac susceptibility and the observations of major peaks below T_C in the CrAlGe system indicate that a cluster glass, or RSG state, exists within the material.

To further explore the glassy behavior in CrAlGe, ac susceptibility data were obtained at ac fields of various

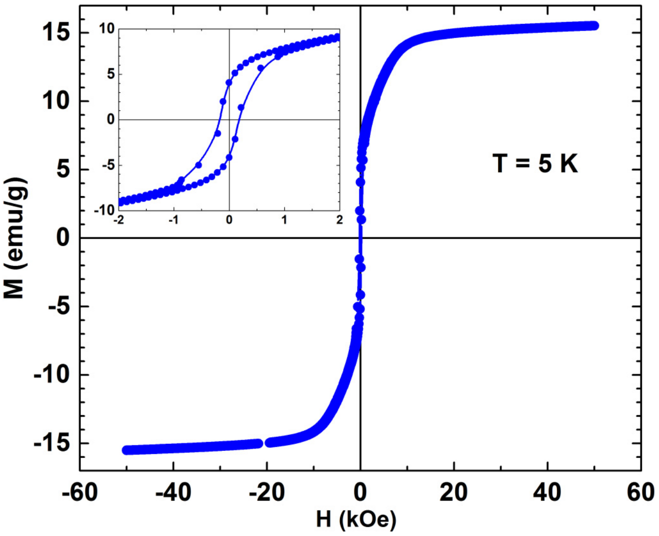

FIG. 8. Field dependence of magnetization for CrAlGe measured at 5 K.

amplitudes as well as at different dc magnetic fields. Figure 10 shows the ac susceptibility data measured as a function of temperature at various ac fields and a frequency of 10 Hz.

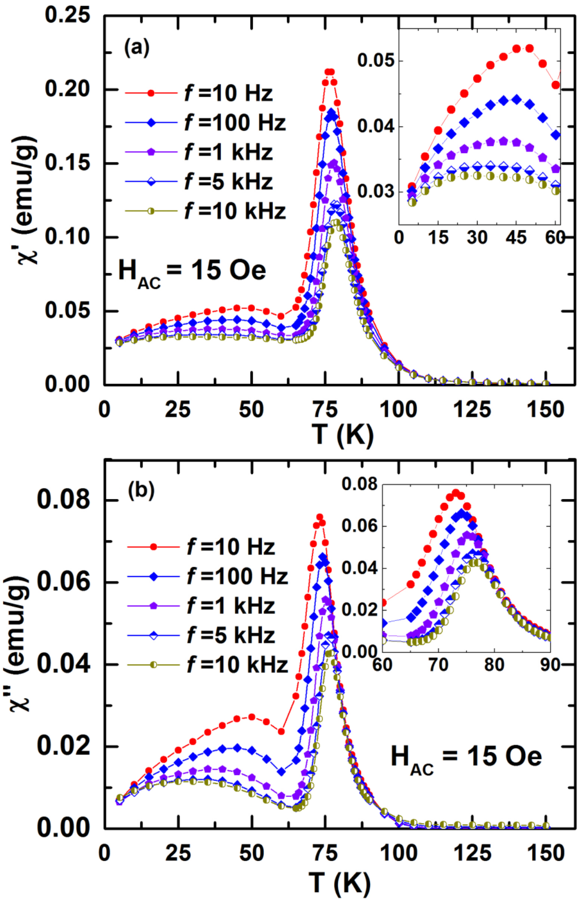

FIG. 9. Temperature dependence of the (a) real (χ') and (b) imaginary (χ'') components of the ac susceptibility for CrAlGe measured at frequencies varying from 10 to 10000 Hz. The insets of the figure show the magnified version of selected regions of the data.

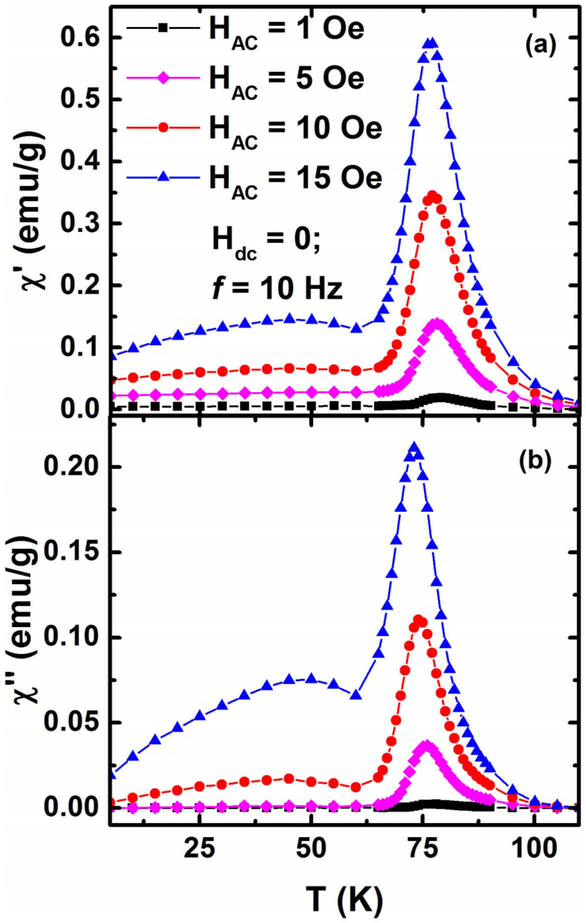

FIG. 10. Temperature dependence of the (a) real (χ') and (b) imaginary (χ'') components of the ac susceptibility for CrAlGe measured at a frequency of 10 Hz and ac field amplitudes varying from 1 to 15 Oe.

As shown in Fig. 10(a), the peak near 76 K in the $\chi'(T)$ shifts to lower temperature from $\sim$79 K ($H_{ac} = 1$ Oe) to $\sim$76 K ($H_{ac} = 15$ Oe), while the magnitude of the peak dramatically increases. The $\chi''(T)$ data exhibit similar behavior where the peak temperature shift from $\sim$77 K ($H_{ac} = 1$ Oe) to $\sim$73 K ($H_{ac} = 15$ Oe). Figure 11 show the real and the imaginary components of the ac susceptibility data obtained at various dc magnetic fields (constant ac field of 15 Oe and $f = 10$ Hz) for CrAlGe. As shown in the figure, for both the $\chi'(T)$ and $\chi''(T)$ data, the $\sim$76 K peak is strongly suppressed with increasing dc magnetic field. For $H_{dc} > 300$ Oe, the peak is completely suppressed. Although the peak is strongly suppressed by the dc field, the peak temperature stays nearly same for all fields. It is also to be noted that below $\sim$60 K, the effect of the dc field on the magnitude of the ac susceptibility (particularly the real component) is relatively less. These observations further confirm the ferromagnetic cluster glass states in CrAlGe [28,29].

Considering that the Cr atoms only occupy a single crystallographic site in the CrAlGe structure, it is unusual to observe spin glass behavior in the material. Therefore, this frustrated magnetic behavior cannot be related to any structural disorder in this phase. One scenario may be taken

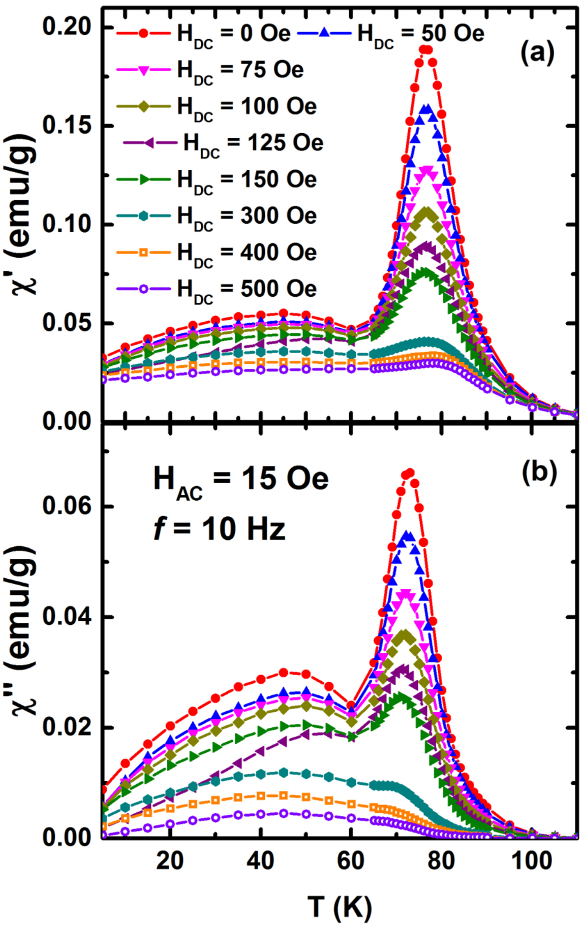

FIG. 11. Temperature dependence of the (a) real (χ') and (b) imaginary (χ'') components of the ac susceptibility for CrAlGe measured at various dc bias fields, a frequency of 10 Hz and at an ac field of 15 Oe.

into consideration to explain the magnetic behavior observed in the CrAlGe compound. It has been reported that when Cr is partially doped with Al in Cr-Al alloys, the *s* and *d* orbitals of Cr hybridize with the *s* and *p* orbitals of Al, which favors antiferromagnetic ordering [30]. On the other hand, Cr-Ge compounds tend to exhibit ferromagnetism [31,32]. For example, $Cr_{11}Ge_{19}$ is ferromagnetic with a T_C of 92 K and exhibits the tetragonal $Mn_{11}Si_{19}$-type structure, where the Cr-Cr interatomic distance is 3.136 Å and the Cr-Ge distance is 2.503 and 2.642 Å [29]. In light of this discussion it is highly possible that if the nearest atom to Cr is Al in CrAlGe, the *sd* orbitals of Cr will hybridize with the *sp* orbitals of Al resulting in AFM-type spin alignment. On the other hand, the Cr-Ge interatomic distance in CrAlGe (ranging from 2.563 to 2.756 Å as shown in Table II) compares well to the Cr-Ge distance in $Cr_{11}Ge_{19}$ [29]. Therefore, a ferromagnetic alignment may be expected. Under these circumstances, a frustrated magnetic structure with competing ferromagnetic and antiferromagnetic interactions will form in the CrAlGe compound that may well explain the coexisting ferromagnetic and spin glass behavior observed in the material. However, to confirm this argument more measurements (such as neutron diffraction) will be necessary.

IV. CONCLUSION

In conclusion, we have investigated the structural, magnetic, and transport properties of CrAlGe, which exhibits the orthorhombic $TiSi_2$-type structure. The ac susceptibility data showed two distinct frequency dependent peaks, which correspond well and corroborate the results obtained from the magnetization and electrical resistance measurements. The ac susceptibility and electrical resistance data strongly demonstrate the coexistence of ferromagnetism and cluster glass type states in the material. These mixed magnetic interactions are formed due to the random occupancy of the Al and Ge atoms on the 16*f* site. When Al is the closest atom to Cr, antiferromagnetic spin alignment is favored, while ferromagnetic alignment is expected when Ge is the closest atom to Cr. Thus, a frustrated magnetic structure is formed in CrAlGe, resulting in the coexistence of ferromagnetism and cluster glass type magnetic states in the compound.

---

[1] E. Fawcett, Rev. Mod. Phys. **60**, 209 (1988).
[2] D. A. Papaconstantopoulos, J. L. Fry, and N. E. Brener, Phys. Rev. B **39**, 2526 (1989).
[3] M. Podgórny and J. Goniakowski, Phys. Rev. B **42**, 6683 (1990).
[4] M. Albrecht, M. Maret, J. Köhler, B. Gilles, R. Poinsot, J. L. Hazemann, J. M. Tonnerre, C. Teodorescu, and E. Bucher, Phys. Rev. Lett. **85**, 5344 (2000).
[5] W. Feng, D. D. Dung, and S. Cho, Phys. Rev. B **82**, 132401 (2010).
[6] S. Yoshinaga, Y. Mitsui, R. Y. Umetsu, and K. Koyama, Phys. Procedia **75**, 918 (2015).
[7] Y. Fukuda and S. Fujii, J. Alloys Compd. **687**, 17 (2016).
[8] J. H. Wernick, S. E. Haszko, and W. J. Romanov, J. Appl. Phys. **32**, 2495 (1961).
[9] H. Ido, T. Kamimura, and K. Shirakawa, J. Appl. Phys. **55**, 2365 (1984).
[10] R. Y. Umetsu, Y. Mitsui, I. Yuito, T. Takeuchi, and H. Kawarada, IEEE Trans. Magn. **11**, 1001904 (2014).
[11] K. Jonason, J. Mattsson, and P. Nordblad, Phys. Rev. Lett. **77**, 2562 (1996).
[12] I. S. Suzuki and M. Suzuki, Phys. Rev. B **73**, 094448 (2006).
[13] D. X. Li, S. Nimori, Y. Shiokawa, Y. Haga, E. Yamamoto, and Y. Onuki, Phys. Rev. B **68**, 172405 (2003).
[14] C. Tien, C. H. Feng, C. S. Wur, and J. J. Lu, Phys. Rev. B **61**, 12151 (2000).
[15] A. A. Belik, N. Tsujii, Q. Huang, E. Takayama-Muromachi, and M. Takano, J. Phys.: Condens. Matter **19**, 145221 (2007).
[16] K. Binder and A. P. Young, Rev. Mod. Phys. **58**, 801 (1986).
[17] K. Yvon, W. Jeitschko, and E. Parthé, J. Appl. Crystallogr. **10**, 73 (1977).
[18] J. Rodriguez-Carvajal, Physica B **192**, 55 (1993), http://www.ill.eu/sites/fullprof/php/downloads.html.
[19] V. V. Milyan and Y. B. Kuz'ma, Russ. Metal. **4**, 191 (1987).
[20] F. Laves and H. J. Wallbaum, Z. Kristallogr. **101**, 78 (1939).

[21] W. Jeitschko, Acta Crystallogr. Sect. B **33**, 2347 (1977).

[22] P. Villars and L. D. Calvert, *Pearson's Handbook of Crystallographic Data for Intermetallic Compounds*, 2nd ed. (OH ASM International, Metals Park, CA, 1991).

[23] P. Villars and K. Cenzual, *Pearson's Crystal Data—Crystal Structure Database for Inorganic Compounds, Release 2010/11* (ASM International, Materials Park, Ohio, 2010).

[24] W. Jeitschko and E. Parthé, Acta Crystallogr. **22**, 417 (1967).

[25] H. Nowotny, *Electronic Structure and Alloy Chemistry of the Transition Elements*, edited by P. A. Beck (Interscience, New York, 1963), pp. 179–220.

[26] E. Teatum, K. A. Gschneidner Jr., and J. Waber, Rep LA-4003, NTIS, Springfield, VA, 1968.

[27] D. X. Li, A. Dönni, Y. Kimura, Y. Shiokawa, Y. Homma, Y. Haga, E. Yamamoto, T. Honma, and Y. Onuki, J. Phys.: Condens. Matter **11**, 8263 (1999).

[28] A. Kumar, R. P. Tandon, and V. P. S. Awana, J. Appl. Phys. **110**, 043926 (2011).

[29] R. C. Sahoo, S. K. Giri, D. Paladhi, A. Das, and T. K. Nath, J. Appl. Phys. **120**, 033906 (2016).

[30] M. Wang, X. Huang, Z. Du, and Y. Li, Chem. Phys. Lett. **480**, 258 (2009).

[31] M. Kolenda, J. Stoch, and A. Szytula, J. Magn. Magn. Mater. **20**, 99 (1980).

[32] S. Choi, S. C. Hong, S. Cho, Y. Kim, J. B. Ketterson, C.-U. Jung, K. Rhie, B.-J. Kim, and Y. C. Kim, Appl. Phys. Lett. **81**, 3606 (2002).